# 193 nm photodissociation of acetylene

B. A. Balko, J. Zhang, and Y. T. Lee

Citation: The Journal of Chemical Physics **94**, 7958 (1991); doi: 10.1063/1.460130
View online: http://dx.doi.org/10.1063/1.460130
View Table of Contents: http://scitation.aip.org/content/aip/journal/jcp/94/12?ver=pdfcov
Published by the AIP Publishing

# 193 nm photodissociation of acetylene

B. A. Balko, J. Zhang, and Y. T. Lee
*Department of Chemistry, University of California at Berkeley and Chemical Sciences Division, Lawrence Berkeley Laboratory Berkeley, California 94720*

(Received 21 January 1991; accepted 4 March 1991)

The product translational energy distribution $P(E_T)$ for acetylene photodissociation at 193 nm was obtained from the time-of-flight spectrum of the H atom fragments. The $P(E_T)$ shows resolved structure from the vibrational and electronic excitation of the $C_2H$ fragment; comparison of the translational energy release for given excited states of $C_2H$ with the known energy levels of these states gives $D_0(HCC-H) = 131.4 \pm 0.5$ kcal/mol. This value is in agreement with that determined previously in this group from analogous studies of the $C_2H$ fragment and with the latest experimental and theoretical work. The high resolution of the experiment also reveals the nature of $C_2H$ internal excitation. A significant fraction of the H atoms detected at moderate laser power were from the secondary dissociation of $C_2H$. The $P(E_T)$ derived for this channel indicates that most of the $C_2$ is produced in excited electronic states.

## I. INTRODUCTION

Although acetylene and the ethynyl radical play important roles in combustion,[1] their energetics and photochemical behavior are not precisely known. The HCC–H bond energy remains controversial and the strong coupling between the $C_2H(A\ ^2\Pi)$ and $C_2H(X\ ^2\Sigma_g^+)$ electronic states makes accurate determinations of the vibrational and electronic transitions difficult.

Five years ago, this group obtained the HCC–H bond energy from the measurement of the translational energy distribution of the $C_2H$ fragments produced by the photodissociation of $C_2H_2$ with 193 nm photons.[2] This value was in agreement with others determined around the same time using different techniques.[3,4] In 1989, however, two groups reported numbers which were significantly lower.[5,6] This brought the acetylene C–H bond energy into question again and initiated a flurry of experimental and theoretical studies[10–13] (see Table I). As one of the lower bond energies was based on the measurement of the H atom translational energy distribution via the Doppler profile,[5] it was decided to measure directly the velocity distribution of H atoms using the molecular beam photofragmentation technique for a comparison. Since the experimental setup can be calibrated for precise velocity measurements of H atoms by photolyzing well-characterized hydrogen halides, any questions regarding systematic errors should be eliminated.

The $C_2H_2$ photodissociation is one instance where having the ability to obtain high resolution time-of-flight (TOF) spectra is worthwhile. The $C_2H$ fragment is not expected to be significantly rotationally excited, so the peaks in the TOF spectrum corresponding to various vibrational and electronic energy levels will not be smeared out. The parent $C_2H_2$ molecules in the beam produced by a supersonic expansion through the nozzle should have a very low rotational temperature, which means rotational excitation of the $C_2H$ fragment can only come from the recoil of the H atom leaving the $C_2H$. Owing to the light mass of the H atom and a relatively small exit impact parameter, the torque exerted to the $C_2H$ product is expected to be small, especially when the H atoms depart with low translational energies. Seeing the internal energy distribution of the $C_2H$ fragments from the $C_2H_2$ dissociation is especially interesting because of the several potential energy surfaces involved[2] and the confusion of states in the $C_2H$ system.[14] In addition, the extensive coupling between the $C_2H$ $A$ and $X$ electronic states means that the Born–Oppenheimer approximation, a standard assumption in many photodissociation models, is not appropriate.[15]

At 193 nm, acetylene is excited to $\nu_3 = 10$ (the C–H bending vibration) of the $^1A_u$ *trans*-bent excited states.[16–18] Figure 1 shows the products that are thermodynamically possible. At laser intensities below $10^{26}$ photons/cm$^2$ s for a pulse duration of approximately 20 ns, the primary process Wodtke and Lee observed[2] is

$$C_2H_2 \rightarrow C_2H + H. \qquad (I)$$

TABLE I. Recent determinations of $D_0$(HCC–H).

| Year | $D_0$(HCC–H) (kcal/mol) | Technique | Reference |
|---|---|---|---|
| 1991 | $131.4 \pm 0.5$ | H atom (mass spectroscopy) velocity after dissociation | This work |
| 1990 | $131 \pm 1$ | H atom (REMPI)[a] velocity after dissociation | 9 |
| 1990 | $131.6 \pm 1$ | $C_2H^- + H^+$ threshold thermochemical cycle | 8 |
| 1990 | $131.3 \pm 0.7$ | Radical electron affinity (photoelectron spectroscopy) + gas phase acidity thermochemical cycle | 7 |
| 1990 | 129.7 | Theory | 13 |
| 1990 | $130.1 \pm 1$ | Theory | 12 |
| 1990 | $131.54 \pm 0.51$ | Theory | 11 |
| 1989 | $126.647 \pm 0.002$ | SAC[b] | 6 |
| 1989 | $<127 \pm 1.5$ | H atom Doppler shifts after dissociation | 5 |
| 1989 | $133.52 \pm 2.3$ | Theory | 10 |
| 1988 | $<132.3 \pm 0.001$ | SEP[c] with ZAC[d] | 4 |
| 1987 | $132.6 \pm 1$ | $C_2H + H^+ + e^-$ threshold thermochemical cycle | 3 |
| 1985 | $132 \pm 62$ | $C_2H$ velocity after dissociation | 2 |

[a] Resonance enhanced multiphonon ionization (REMPI).
[b] Stark anticrossing spectroscopy (SAC).
[c] Stimulated emission pumping (SEP).
[d] Zeeman anticrossing spectroscopy (ZAC).

 0021-9606/91/127958-09$03.00 

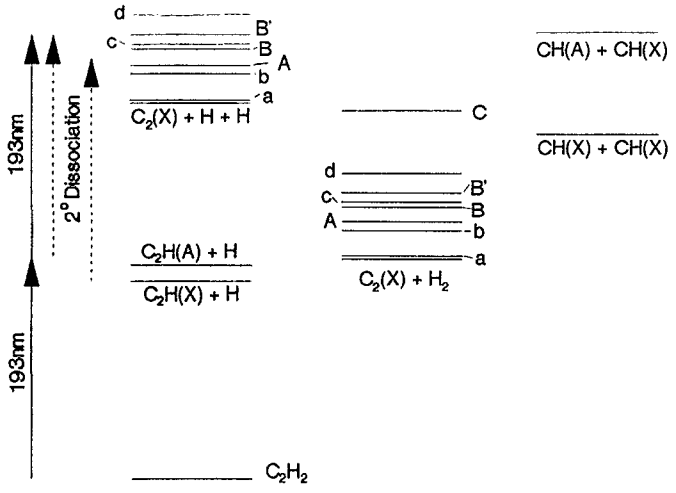


FIG. 1. Product channels thermochemically possible in the 193 nm photodissociation of acetylene. The dashed, secondary dissociation lines represent the energy limits if the ground state or the most internally excited $C_2H$ absorbs a photon. The heats of formation and bond energies used to construct this chart are from Refs. 7 and 19–21.

Because of the large changes in the equilibrium C–C bond lengths and C–C–H bond angles that occur during the dissociation process, they suggested that the $C_2H$ C–C stretch and C–H bend will be excited.[2] In their Fourier transform infrared (FTIR) study of the $C_2H$ products, Fletcher and Leone determined that the ethynyl radical was formed in both the $A$ and $X$ electronic states and was indeed highly vibrationally excited.[22] No evidence has been found for the only other one-photon channel thermodynamically allowed

$$C_2H_2 \rightarrow C_2 + H_2. \qquad \text{(II)}$$

Wodtke and Lee did not detect $C_2$ from this channel, but estimated that it could be as much as 15% of channel I and still remain hidden in the signal from $C_2$ formed in the secondary photodissociation of $C_2H$.[2]

At higher laser intensities, more channels open up. The early emission studies of McDonald, Baronavski, and Donnelly on the multiphoton photodissociation of $C_2H_2$ identified several processes from two- and three-photon absorption. Most ($\geqslant$90%) of the measured emission intensity was from the $C_2(A\,^1\Pi_u \rightarrow X\,^1\Sigma_g^+)$ transition. Their observations were consistent with a two-photon process that proceeds via sequential elimination of two H atoms

$$C_2H_2 \rightarrow C_2H + H, \quad C_2H \rightarrow C_2 + H.$$

Emission from $C_2(d\,^3\Pi_g \rightarrow a\,^3\Pi_u)$ was also detected, but this was only a minor channel ($\sim$1% of the $A\,^1\Pi_u$); based on lifetime measurements and the power dependence, they concluded that three photons were absorbed, but could not determine the mechanism. Fluorescence from $CH(A\,^2\Delta \rightarrow X\,^2\Pi)$ was recorded as well; this channel was also minor ($<$1% of $A\,^1\Pi_u$). The production of $CH(A_2\Delta)$ appeared to proceed via two-photon excitation of $C_2H_2$—the $C_2H$ intermediate was not involved. Finally, emission from $C_2(C\,^1\Pi_g \rightarrow A\,^1\Pi_u)$ was reported, but the signal was not intense enough ($<$1% of $A\,^1\Pi_u$) to derive any mechanistic information.[23] $C_2(A\,^1\Pi_u, a\,^3\Pi_u, X\,^1\Sigma_g^+)$ was detected by Wodtke and Lee and was shown to have formed after two sequential one-photon absorption steps $C_2H_2 \rightarrow C_2H \rightarrow C_2$.[2] Recently, several more electronically excited $C_2$ states have been observed in the 193 nm photolysis of $C_2H_2$. Using laser-induced fluorescence (LIF) methods, Urdahl, Bao, and Jackson reported the formation of $C_2(a\,^3\Pi_u, d\,^3\Pi_g, A\,^1\Pi_u, C\,^1\Pi_g$, and $B'\,^1\Sigma_g^+)$.[24,25] Goodwin and Cool detected $C_2(B\,^1\Delta_g)$ and $C_2(b\,^3\Sigma_g^-)$ in the two-step photolysis of $C_2H_2$.[26]

The formation of some of these higher excited states of $C_2$ is only energetically possible if the intermediate $C_2H$ is internally excited. In fact, by studying the change in shape of the $C_2H$ TOF spectra with laser power, Wodtke and Lee showed that the $C_2H$ absorption cross section was larger for more highly excited $C_2H$ molecules.[2] From what is known about the $C_2H$ radical excited electronic states, this is not surprising. The lowest lying electronic states for which a transition from the $^2\Sigma^+$ ground state is allowed are $^2\Sigma^+$ and $^2\Pi$. These states have vertical excitation energies of 7.32 and 8.11 eV, respectively. The transition energy, however, drops to the 193 nm range if one assumes that the upper state is bent in its equilibrium configuration and that the initial state's C–C bond length is greater than the equilibrium value and/or the C–C–H angle is not 180°.[14,27,28]

## II. EXPERIMENT

In reinvestigating the 193 nm photodissociation of acetylene, the same method—photofragmentation translational spectroscopy—is used, but the H atom studies are done with a high resolution fixed source/rotating detector molecular beam apparatus.[29] This machine was recently modified to allow the use of a pulsed photolytic beam source (see Fig. 2).[30] Briefly, a homemade piezoelectric pulsed valve fires into a small chamber pumped by a 4 in. diffusion pump and a liquid nitrogen cooled cryopanel. The focused output of an ArF Lambda Physik 202 MSC ILC excimer laser enters this chamber, crossing the molecular beam perpendicularly. For higher resolution studies, a skimmer can be inserted between the pulsed valve nozzle and laser interaction region to reduce the angular spread of the acetylene beam. The photoproducts are detected by a mass spectrometer which is perpendicular to the $C_2H_2$ beam direction at a distance of 39.0 cm from the photolysis region.

This experimental arrangement has several advantages over that of Wodtke and Lee which are obvious from the kinematic diagrams in Fig. 3. First, since the product angular distribution is isotropic,[2] by detecting the fast H atoms, the entire product energy distribution can be obtained at one laboratory angle. Second, detection of the fast product has inherently better resolution because the H atom velocity distribution will not be significantly perturbed by the spread in parent beam velocities and angles. This makes it possible to use a beam which is less defined, but with a much higher intensity to increase the experimental signal-to-noise ratio (S/N). Finally, as the detector axis is 90° from the $C_2H_2$ beam, there will be less background from the dissociative ionization of the parent molecules, which is a problem at lab angles close to the beam where Wodtke and Lee were forced to go to in order to see the slow $C_2H$ products.

Of course, H atom detection has its own disadvantages. The very low energy tail ($<$3 kcal/mol) of the product

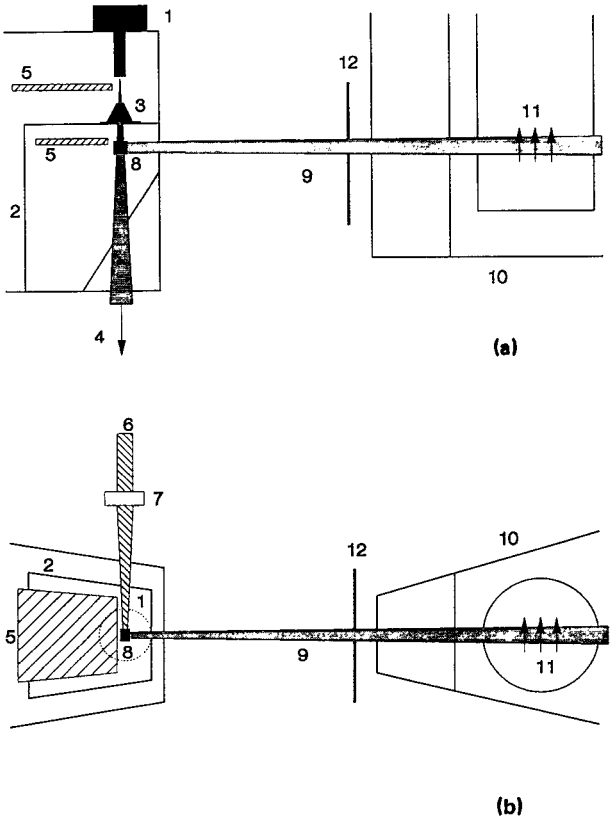


FIG. 2. (a) Side view and (b) top view of the experimental arrangement. The piezoelectric pulsed valve (1) is used to create a beam of $C_2H_2$. The valve fires into the photolysis chamber (2). The beam passes through a skimmer (3) in the high resolution mode. A 4 in. diffusion pump (4) as well as liquid nitrogen cooled cryopanels (5) pump the chamber. The output of the excimer laser (6) passes through a focusing lens (7) and perpendicularly intersects the acetylene beam (8). The photoproducts (9) pass out the differential chamber and travel 39.0 cm to the detector (10), where they can be ionized in the electron impact ionizer (11). A chopping wheel (12) is used to gate the detector to help reduce the background.

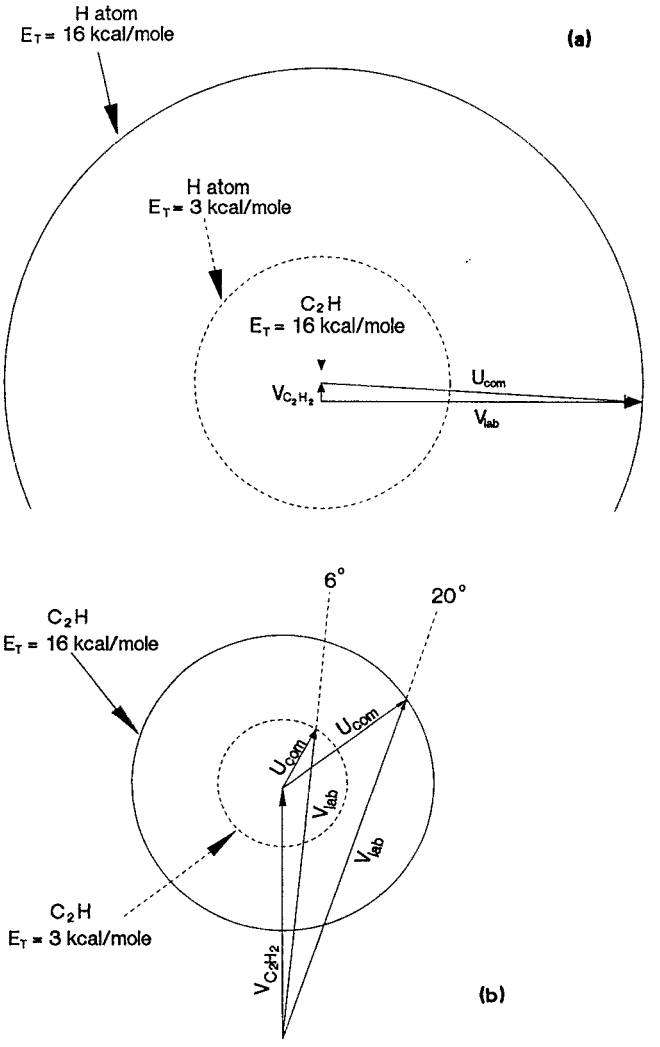


FIG. 3. (a) A kinematic diagram for the experiment showing the H atom product velocity. Sixteen kcal/mol is the translational energy of the fastest $C_2H + H$ products and 3 kcal/mol is the lower limit for most of the observed product. The diagram shows that since the detection direction is perpendicular to the parent beam, the fastest $C_2H$ product cannot be observed. (b) A kinetimatic diagram for Wodtke and Lee's experiment in which they detected the $C_2H$ fragment. A comparison of the two diagrams shows that the present experiment will be much less affected by variations in the parent beam.

translational energy distribution cannot be well determined. The problem is the slow temporal background from the dissociative ionization of the thermalized parent pulsed beam in the detector. The interference from this background, however, is minimized by recording a laser-off TOF spectrum and subtracting it from the laser on (see Fig. 4). Of more concern is contamination from secondary dissociation events; H atoms can come from the primary process $C_2H_2 \rightarrow C_2H + H$, or the secondary $C_2H \rightarrow C_2 + H$. Finally, fast H atoms are more difficult to count. At the low quadrupole rf voltages necessary for mass selection of the H atoms, there is a problem with laser rf pickup causing a time-dependent variation in the transmission of the quadrupole mass filter. Experimentally, this is manifested as large background fluctuations in the TOF scans at short times within the rising edge of the photofragmentation signal used to determine the bond energy. The immediate solution was to record the modulation separately and subtract this signal away (see Fig. 5). Later, an rf power filter (Corcom EMI 10VR7) was installed on the mass spectrometer controller ac input line which essentially eliminated this noise. Another difficulty is that the mass spectrometric detection of H atoms is less sensitive. This is both because the H atom is fast, which limits their residence time in the electron bombardment ionizer, and because the ionization cross sections for H atoms are smaller than for larger molecules such as $C_2H$.[31]

The data discussed here were collected under several different conditions. In all the work, however, the 50 Hz pulsed beam was formed by passing $C_2H_2$ (Matheson) through a dry ice/acetone trap and into the piezoelectric pulsed valve (1 mm diameter nozzle) at a stagnation pressure of 30–75 Torr. In the low resolution experiments, the laser crossed the molecular beam approximately 3 mm from the nozzle. High resolution experiments were also done by inserting a skimmer which increased the nozzle/laser distance to 2.3 cm. To reduce the $m/e = 1$ background, the

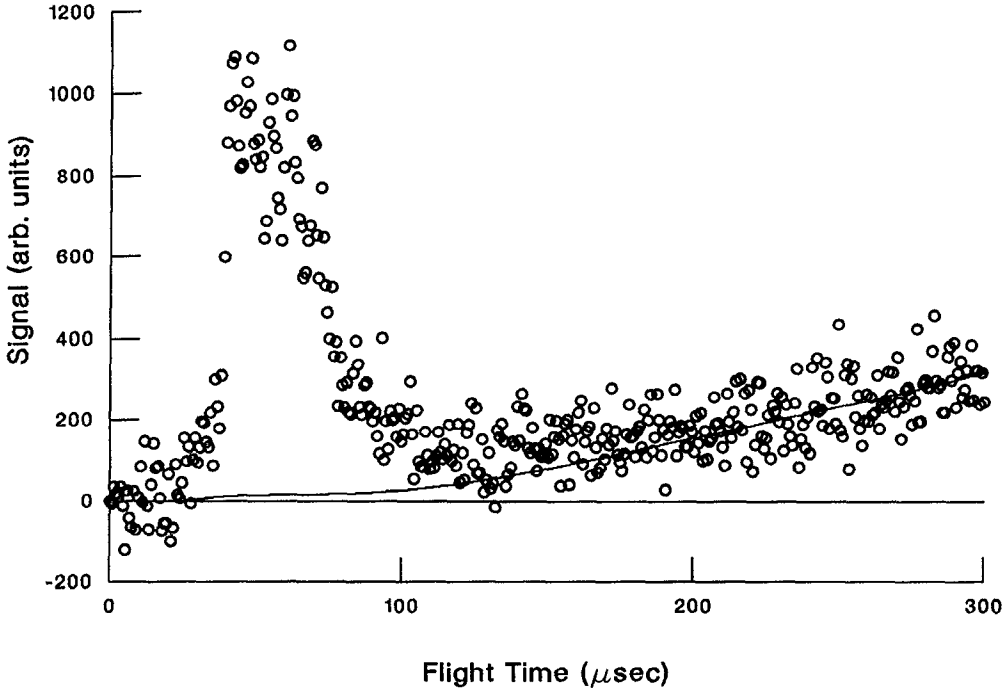


FIG. 4. A representative high resolution TOF spectrum showing the raw data (open circles) as well as the polynomial fit to the laser-off signal (solid line). This background correction has very little effect on the region of interest.

detector opening was gated with a two-slot wheel spinning at 25 Hz which left the detector open for $\approx$400 $\mu$s after the laser irradiation and kept it closed until the next laser pulse. Typically, the laser was focused to a $3\times5$ mm spot at the interaction region with a 30 cm spherical Suprasil lens. The pulse energies used ranged from 20 to 235 mJ/pulse (which correspond to $7\times10^{24}$ and $8\times10^{25}$ photons/cm$^2$ s for the 20 ns pulse); these values are "before lens." A new, clean lens could typically transmit $\sim$90% of the laser power; after a set of experiments, the lens' transmission would drop to $\sim$70% as a result of photolysis by-product buildup. Because this means the laser power at the interaction region varies over time, the laser powers given are what is measured before the lens. A mixture of HI and DI synthesized in the lab[30] was dissociated under these same conditions to permit calibration of the TOF measurements of the H atoms.

Once the TOF spectra were obtained, the raw data was corrected for the pulsed valve temporal background and rf pickup. A forward convolution data analysis program[32] was used to fit the HI and DI TOF spectra. An input translational product energy distribution $P(E_T)$ was generated using the photon energy along with the known bond energies and iodine excitation energies. The program then averaged this over experimental variables (parent beam velocity,

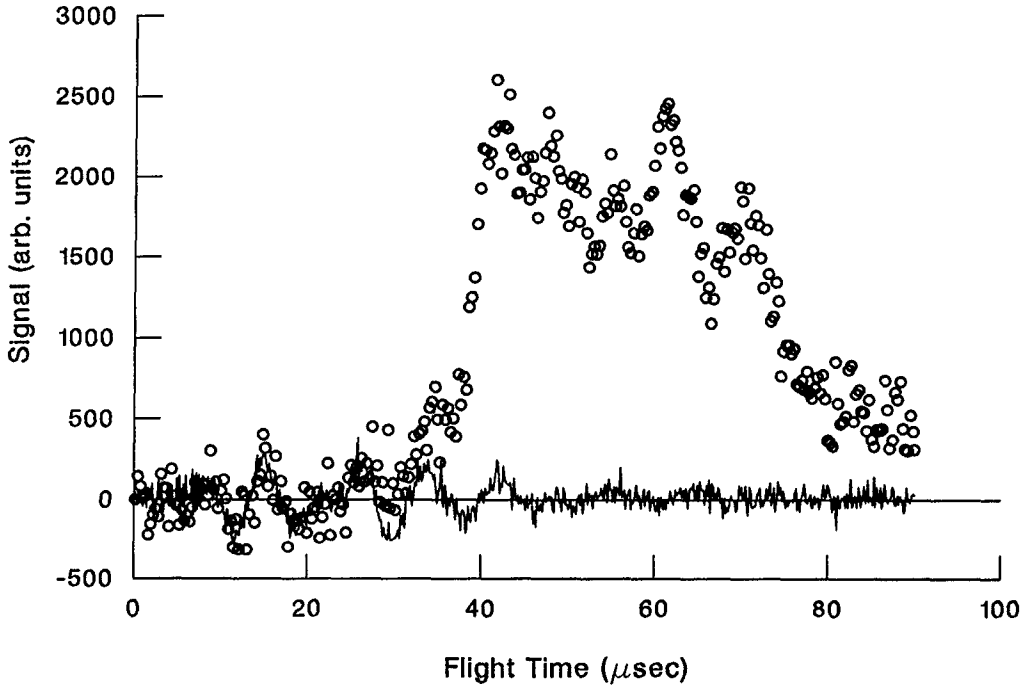


FIG. 5. A representative high resolution TOF spectrum showing the raw data (open circles) with the rf pickup noise spectrum (solid line).

beam spread, detector viewing angle, and laboratory angle); with fine adjustments of the detector parameters (ion flight time, effective length of ionizer, and product flight length), good fits to these TOF spectra were obtained. These final values were then used in fitting the H atom spectra from the $C_2H_2$ photodissociation. Using an iterative process, the input $P(E_T)$ was adjusted until the calculated TOF agreed with the experimental.

## III. RESULTS

### A. Calibration

Figure 6 shows the H and D atom spectra from the photodissociation of a skimmed and unskimmed beam of HI and DI. The solid line is the best fit TOF spectra assuming an initial parent rotational temperature of 100 K. Because of the substantial translational energy release, the fits are not sensitive to this temperature; the peak width is mainly a function of the ionizer length and photolysis volume. The differences between spectra with and without the skimmer should be noted. Without the skimmer to help define the beam, the photolysis region is larger, so there is more spread in the H atom flight length which broadens the peaks.

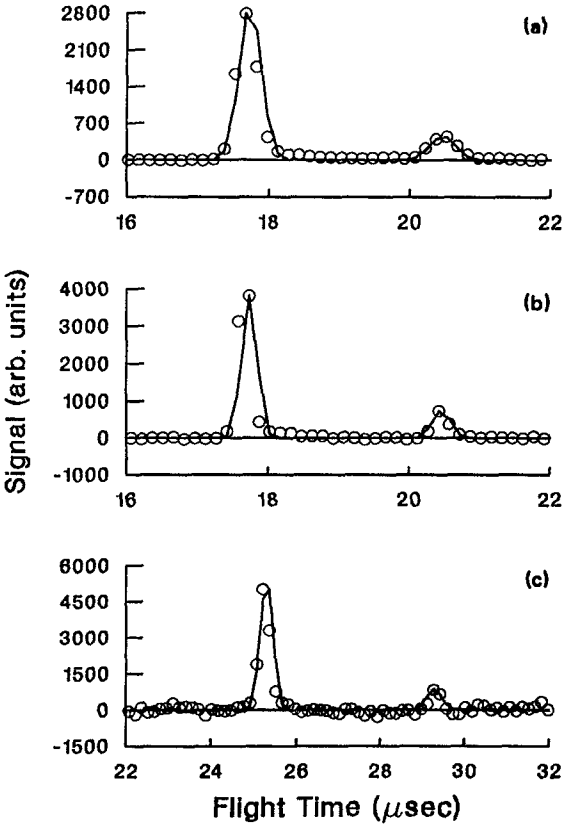


FIG. 6. H/D atom TOF spectra from HI/DI photolysis for calibration purposes. The two peaks in each spectrum are due to the formation of $I(^2P_{3/2})$ and $I(^2P_{1/2})$. Open circles are the raw data and the solid line is the calculated fit. Photodissociation of (a) HI in the low resolution mode; (b) HI in the high resolution mode; and (c) DI in the high resolution mode (note the change in time scale).

### B. Skimmed beam/high resolution

As discussed previously, one of the problems in determining the HCC–H bond dissociation energy with the H atom TOF technique is the possibility of contamination from secondary dissociation events which can produce fast H atoms. The TOF spectrum shown in Fig. 7(a) which is mainly due to the single-photon dissociative process could only be obtained at very low laser powers ($\sim$35 mJ/pulse). Despite 5.6 h of counting, the S/N ratio of the spectrum is still low; the scan, however, is of sufficient quality to generate the fast edge of the $P(E_T)$, which can then be incorporated in fitting spectra where secondary dissociation is more of a problem.

To get sufficient S/N to resolve the vibrational and electronic states of the $C_2H$ radical, higher laser powers ($\sim$100–150 mJ/pulse) were required. Figure 7(b) shows the accumulated spectrum after the runs have been added (21 h) and all background/rf noise corrections made. The solid line is the TOF calculated using the $P(E_T)$ in Fig. 8(a). The dashed line represents the products from the secondary dissociation, the details of which are discussed later. Comparing the $P(E_T)$ derived from the H atom TOF with that of Wodtke and Lee shows good general agreement [see Fig. 8(b)]. As anticipated, however, the resolution of the former is higher. Most notably, Wodtke's peak 2 appears as two separate peaks.

### C. No-skimmer/low resolution

When photolyzing in the free jet, a good deal of product vibration/electronic state resolution is lost partly due to

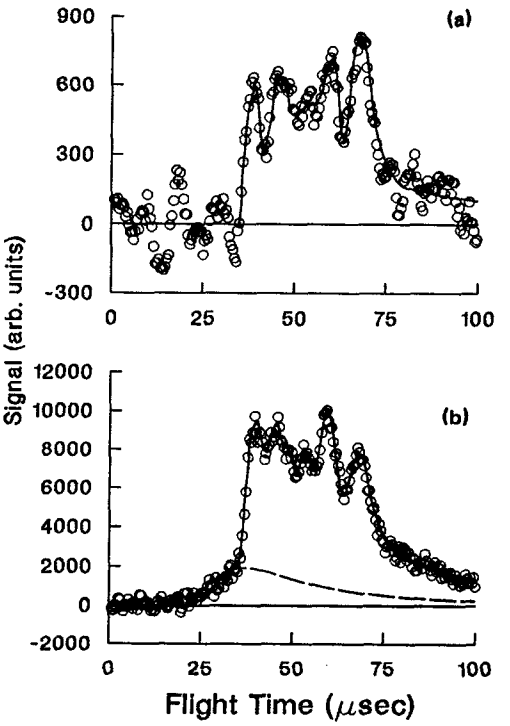


FIG. 7. High resolution H atom spectra. Open circles are the raw data (after background corrections) and the solid line is the calculated best fit. The dashed line represents H atoms from secondary dissociation. (a) Low power, 35 mJ/pulse; (b) high power, 100–150 mJ/pulse.

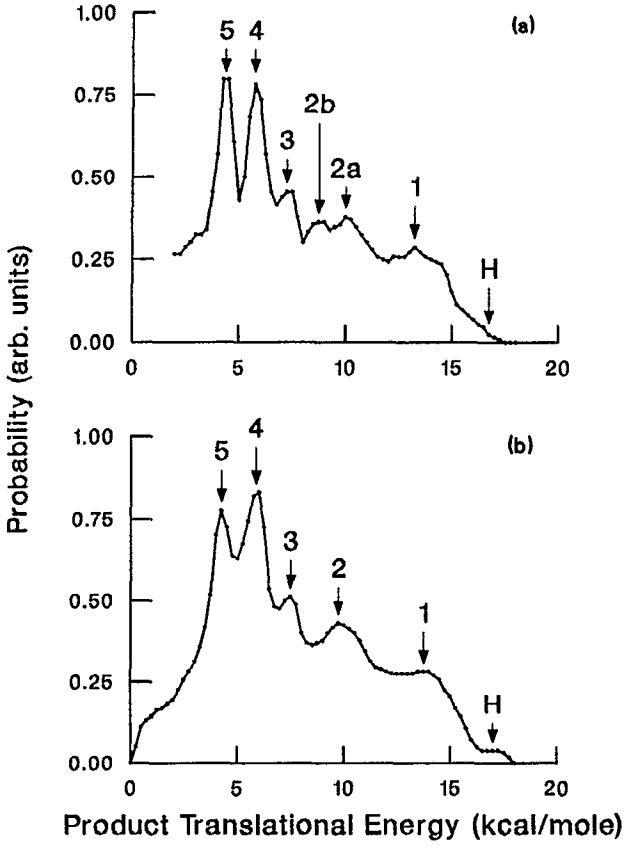


FIG. 8. (a) Product translational energy distribution used to fit the TOF spectrum in Fig. 7(b). (b) Wodtke and Lee's product translational energy distribution that gives the best fit to their $C_2H$ TOF spectra.

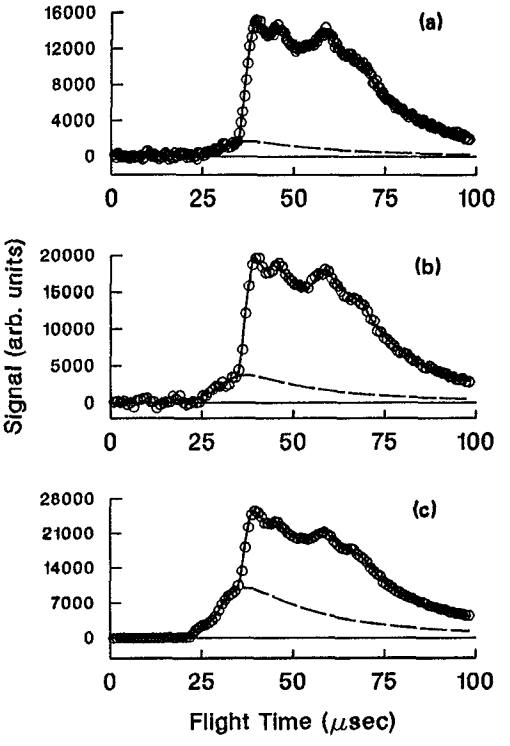


FIG. 9. Low resolution TOF spectra. Open circles are the raw data, solid lines are the calculated best fit, and dashed lines are the secondary dissociation contribution. (a) 60 mJ/pulse; (b) 105 mJ/pulse; (c) 235 mJ/pulse.

collisional broadening, making these spectra less useful for determining the internal energy distribution of the primary products. The S/N ratio, however, is much higher, which means less counting time is necessary so laser power dependence studies become practical.

Figure 9 shows three low resolution H atom TOF spectra taken at different laser powers ($\sim$60, 105, and 235 mJ/pulse). All the H atoms are either from the primary process $C_2H_2 \rightarrow C_2H + H$, or from the secondary process $C_2H \rightarrow C_2 + H$. There is much uncertainty in fitting the secondary event. One cannot presume that all $C_2H$ formed has the same probability of undergoing secondary photodissociation. In fact, Wodtke and Lee have suggested that more highly internally excited products absorb a photon much more readily.[2] The forward convolution fitting of the power dependence allows one to establish limits on the internal energy requirement. For ease in calculations, the dependence of the secondary dissociation on the primary product internal energy was treated as a step function. The differences between the high and low power TOF spectra indicate that $C_2H$ fragments formed with $E_T \geqslant 10$ kcal/mol do not dissociate. There is enough uncertainty, however, in the comparison that this should be considered an upper bound. In fact, with the assumption that only $C_2H$ with $E_T \leqslant 10$ kcal/mol would be able to fragment ($E_{T,\text{thres}} = 10$ kcal/mol), it was impossible to simulate the "dip" on the rising edge of the high power TOF spectrum. Using $E_{T,\text{thres}} = 7$ kcal/mol proved most successful.

The secondary $P(E_T)$ that best fits the spectra is shown in Fig. 10. The overall appearance—the bimodal distribution and the preference for formation of slow, highly internally excited $C_2$—is unquestionable. There is, however, uncertainty in the shape of the curves, especially at lower translational energies which describes secondary products arriving at the detector at the same time primary products do and at the maximum translational energy where it is difficult to determine exactly at what point the signal disappears.

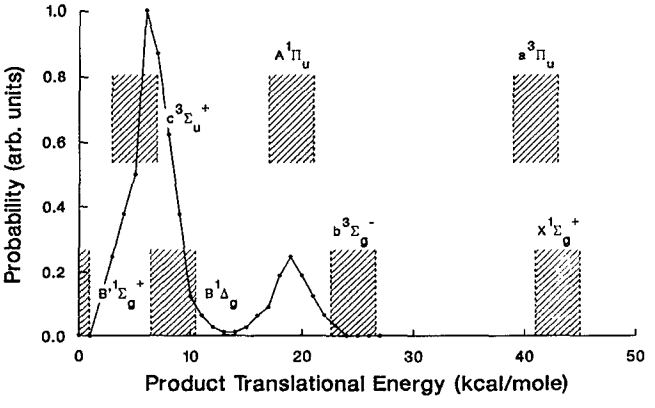


FIG. 10. Secondary dissociation product translational energy distribution used to calculate the best fit in Fig. 9(c). The blocks represent where the ground vibrational level of the $C_2$ electronic states should appear assuming $C_2H$ with an internal energy of 9.5–13.5 kcal/mol ($E_T = 3$–7 kcal/mol) dissociates.

## IV. DISCUSSION

### A. Primary dissociation

The fast edge of the $P(E_T)$ which is where ground state $C_2H$ is expected begins at $E_T = 17.5$ kcal/mol corresponding to a bond energy of 130.4 kcal/mol. Comparing the $P(E_T)$ with that of Wodtke and Lee, however, shows that this fast edge has contamination from photodissociation of internally excited $C_2H_2$.[2] The recent work identifying $C_2H$ vibrational and electronic states provides an alternative to estimating where the ground state $C_2H_2$ dissociation actually starts contributing, reducing the uncertainty in this bond energy measurement. The maximum translational energy of the ground state $C_2H$ product is determined by matching the sharp structures shown as peaks 4 and 5 in the $P(E_T)$ with the known $C_2H$ energy levels. Since an inverted vibrational distribution with selective excitation of only two higher vibrational states of the ground electronic state is not likely, it was assumed that these peaks correspond to electronically excited $C_2H$ in the $A$ state. The main uncertainty in the fitting ($\sim \pm 0.5$ kcal/mol) comes in deciding how much rotational excitation to include. Not much excitation is expected at this low translational energy; in fact, in their study, Fletcher and Leone calculate the average energy in rotation for the $C_2H$ $A$ (0 1 0) to be 0.45 kcal/mol.[22] Table II and Fig. 11[33–39] show the final fit. Accepting that the $P(E_T)$ peaks are correctly assigned, the $C_2H$ ground state is associated with a product translational energy of 16.5 kcal/mol; $D_0$(HCC–H) would then be $131.4 \pm 0.5$ kcal/mol.

The $P(E_T)$ consists of three envelopes. The first $E_T \sim 11.5$–16.5 kcal/mol could only be from the C–H bending series $\nu_2 = 0$–5 using Kanamori and Hirota's $\omega_e\chi_e = 10.1\,\mathrm{cm}^{-1}$ along with their (0 7 0) 2166 $\mathrm{cm}^{-1}$ peak assignment[36] to predict the frequencies of the other bending overtones. The next step in the $P(E_T)$, $E_T \sim 8$–11.5 kcal/mol, is associated with the excitation of the C–C stretch. By analogy, the last grouping $E_T \sim 2$–8 kcal/mol should be $C_2H$ with the C–H stretch excited as well as $C_2H$ in the $A$ state. This assignment would suggest that the C–H stretching fundamental was near 3000–3150 $\mathrm{cm}^{-1}$ ($E_T = 7.5$–8 kcal/mol). $\nu_1$ is still a subject of controversy; currently, the only limitations placed on it are that it fall in the 3250–3620 $\mathrm{cm}^{-1}$ range.[37,40] The pattern in the $P(E_T)$ presented here indicates that $C_2H$ $\nu_1$ is at the lower end of the expected values.

TABLE II. Observed $C_2H$ states and their positions in the $P(E_T)$.

| TOF peak | Exp. trans. ($\mathrm{cm}^{-1}$) | Assignment | Reference |
|---|---|---|---|
| | 5543 | | |
| | 5403 | | 33,34 |
| | 5161 | $X$ | |
| | (from 3320 + $\nu_3$) | | 33 |
| 5 | 4144 | $A$(0 1 0) | |
| | 4108 | $X$(0 1 2) | 15,34,35 |
| | 4012 | $X$(1 1 0) | |
| 4 | 3786 | $X$(0 5 1) | 15,35 |
| | 3693 | $A$(0 0 0) | 15,35,36 |
| | 3600 | | 33,34,36 |
| | 3547 | ?←$X$(0 0 0) | 37 |
| 3 | 3366 | | |
| | 3299 | ?←$X$(0 0 0) | 37 |
| 2*a* | 2166 | $X$(0 7 0) | 36 |
| | 2091 | $X$(0 1 1) | 38 |
| | 1841 | $X$(0 0 1) | 39 |
| 1 | 372 | $X$(0 1 0) | 36 |

Since the acetylene bond energy is dependent on the correctness of the $P(E_T)$ assignment, it is important to consider other possible identification schemes, especially those that would yield lower bond energies. These fits, shown in Fig. 12, are not as satisfying as the $D_0 = 131.4$ kcal/mol one for several reasons. First, they all leave a peak unassigned. Jacox and Olson, however, have seen lines associated with $C_2H$ in these regions,[40] so this is not an entirely convincing argument. A more damaging point is that these fits would require a highly specific and inverted vibrational distribution. For example, with $D_0 = 127.6$ kcal/mol, the three strongest peaks would correspond to high $X$ and/or $A$ vibrational levels. While it is not surprising to find highly vibrationally excited product, such an inversion would not be expected. Finally, the fits at these lower bond energies are not as good. For $D_0 = 130.4$ and 127.6 kcal/mol, $X$(0 7 0), $X$(0 1 1), and $X$(0 0 1) do not match any peaks. This cannot be easily explained by invoking rotational excitation since not much is expected.

The association of the peaks in the $P(E_T)$ with $C_2H$ states does more than determine the translational energy at which the ground state is formed. It also provides dynamic details of the photodissociation process. Although it is impossible to get relative weights for the $C_2H$ states because of their extensive overlap, the general trend is that $C_2H$ with a large amount of internal excitation (8–13 kcal/mol) is preferentially formed. The C–H bend is highly excited as are both the C–C and C–H stretches. The first $C_2H$ electronic state $A\ ^1\Pi_u$ is also reached. As discussed, the large amount of vibrational excitation is expected (especially the C–H bend and C–C stretch) since there are significant changes in the C–C–H bond angle and C–C distance during the dissociation. It is also not surprising to find that $C_2H(A)$ is produced since at 193 nm $C_2H_2$ is excited to the $1\ ^1A''$ state ($C_s$ symmetry) which correlates with $C_2H(A) + H$. In fact, to explain the formation of $C_2H(X)$, one must invoke surface hopping at a $2\ ^1A'/1\ ^1A'$ or a $2\ ^3A'/1\ ^3A'$ avoided crossing.[2,41]

### B. Secondary dissociation

Assuming that primarily $C_2H$ with internal energy of 9.5–13.5 kcal/mol (products with 3–7 kcal/mol in translation) will undergo secondary dissociation to $C_2 + H(^2S)$ and that the H–CC bond energy is 116 kcal/mol,[8,42] the two peaks in the secondary $P(E_T)$ indicate that $C_2$ forms with $E_{int} = 20$–28 (peak 1) and 32–40 kcal/mol (peak 2). Unfortunately, because of the nature of $C_2H$ secondary dissociation, the TOF spectra are not sensitive enough to tell unambiguously what $C_2$ states form. The spectra, however, do

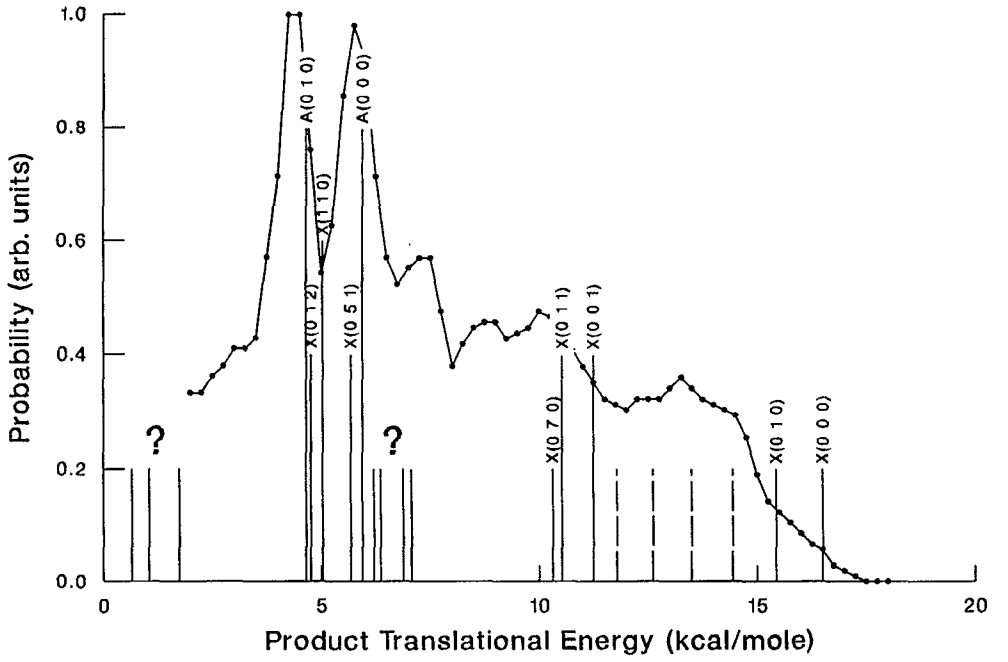


FIG. 11. Correspondence between known $C_2H$ states (see Table II) and the product translational energy distribution. Solid lines are observed transitions (from ground state $C_2H$); those that have been assigned are labeled. The dashed lines are the calculated $C_2H$ C–H bending vibrations assuming Kanamori and Hirota's 2166 $cm^{-1}$ peak is $X$ (0 7 0) and $\omega_e\chi_e = 10.1\ cm^{-1}$ (Ref. 36). As can be seen, $C_2H$ $X$ (0 0 0) is expected at $E_T = 16.5$ kcal/mol, which would yield a $D_0(HCC\text{-}H) = 131.4 \pm 0.5$ kcal/mol.

reveal some general features of the dissociation process.

One conclusion that can be drawn from the secondary dissociation fitting is that $C_2H$ must have an $E_{int}$ of $\geqslant 9.5$ kcal/mol to photodissociate further. This value suggests that only $C_2H$ in the upper electronic $A$ state and/or highly vibrationally excited ground state can absorb a photon and fragment. This would agree with the theoretical predictions of what $C_2H$ electronic transitions are accessible to a 193 nm photon. As discussed, to reach the lowest allowed electronic states, $C_2H$ must have a nonequilibrium C–C bond length and/or be nonlinear.

The overall appearance of the secondary $P(E_T)$ shows that most of $C_2$ is formed highly excited. This is probably because of the large number of $C_2$ electronic states available for the $C_2H^*$ to cross into. Peak 2 most likely represents $B\,^1\Delta_g$ formation with the slow tail being higher vibrational levels of $c\,^3\Sigma_u^+$ and/or $B'\,^1\Sigma_g^+$. The fast edge of peak 1 could be from $b\,^3\Sigma_g^-$ and the slow edge from $A\,^1\Pi_u$. The $C_2$ electronic states that appear to form in the 193 nm secondary dissociation of $C_2H_2$, with the exception of the $c\,^3\Sigma_u^+$ state, have been seen before. The new information these results provide is that more of the highly excited $C_2$ states ($B$, $B'$, and $c$) form than $A$, $a$, or $X$.

## V. CONCLUSION

To confirm this group's previous measurement of the HCC–H bond energy, the same approach, 193 nm photofragmentation translational spectroscopy, was used, but with the H atom detection rather than $C_2H$. Although H atom detection is much more difficult, it has several advantages—the measurements can be well calibrated, the data can be collected at one lab angle, and the TOF spectra are not affected by small variations in the parent beam. Several years

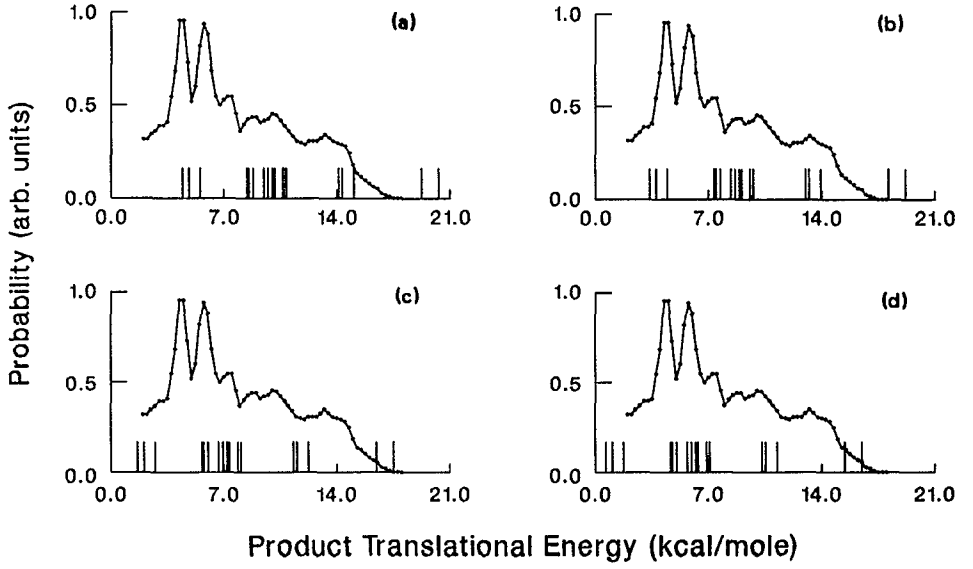


FIG. 12. Comparison of fits of the $C_2H$ spectrum to the H atom TOF spectrum which would give HCC–H bond energies of (a) 127.6; (b) 128.7; (c) 130.4; and (d) 131.4 kcal/mol.

of research on $C_2H$ vibrational and electronic states have made it possible to accurately fix the threshold translational energy of ground state $C_2H$ from the structure of the translational energy distribution rather than having to interpolate where the signal from the dissociation of vibrationally excited $C_2H_2$ ends. These improvements should give confidence in the dissociation energy measured $131.4 \pm 0.5$ kcal/mol. This bond energy agrees with Wodtke and Lee's analogous experiment and is in the range of the latest experimental and theoretical predictions, so it adds more support to the $D_0(HCC-H) > 130$ kcal/mol "side." There was no evidence of the faster primary H atoms as detected in Segall *et al.*'s experiment.

Although the H atom TOF spectra obtained do not have nearly the resolution found in the $C_2H$ absorption spectroscopy studies, $C_2H$ states that lack oscillator strength can be detected. The three vibrational envelopes one can superimpose on the $P(E_T)$ suggest that the C–H stretching fundamental is 3000–3150 $cm^{-1}$, the lower end of the currently accepted range.

Finally, this TOF study adds to the understanding of the 193 nm photodissociation dynamics of acetylene. Comparison to the known $C_2H$ spectrum shows that both $C_2H$ $A$ and $X$ are formed, which is only possible if curve crossing is important in the system. As expected from the large geometry changes involved, high vibrational levels of $C_2H$ $X$ and $A$ are populated. In addition to the primary photodissociation, the results increase what is known about the two-photon sequential dissociation $C_2H_2 \rightarrow C_2H + H \rightarrow C_2 + H + H$. Highly excited $C_2H$ molecules dissociate preferentially as theoretically predicted. The formation of electronically excited $C_2$ is preferred probably because of the large density of these states near the second photon energy.

## ACKNOWLEDGMENTS

The authors would like to thank Professor W. M. Jackson for his useful discussions on the primary and secondary photochemistry processes and for providing a preprint of his group's experimental results. Helpful discussions on experimental techniques and setup with Dr. R. E. Continetti are also acknowledged. This work was supported by the Director, Office of Basic Energy Sciences, Chemical Sciences Division of the U. S. Department of Energy under contract No. DE-AC03-67SF00098.

[1] M. B. Colket III, *Twenty-First Symposium (International) on Combustion* (Combustion Institute, Pittsburgh, 1986), p. 851; C. K. Westbrook and F. L. Dryer, *Eighteenth Symposium (International) on Combustion* (Combustion Institute, Pittsburgh, 1981), p. 749; H. G. Wagner, *Seventeenth Symposium (International) on Combustion* (Combustion Institute, Pittsburgh, 1979), p. 3; T. Tanzawa and W. C. Gardiner Jr., *ibid.*, p. 564.
[2] A. M. Wodtke and Y. T. Lee, J. Phys. Chem. **89**, 4744 (1985); A. M. Wodtke, Ph.D. thesis, University of California, Berkeley, 1986.
[3] H. Shiromaru, Y. Achiba, K. Kimura, and Y. T. Lee, J. Phys. Chem. **91**, 17 (1987).
[4] Y. Chen, D. M. Jonas, C. E. Hamilton, P. G. Green, J. L. Kinsey, and R. W. Field, Ber. Bunsenges. Phys. Chem. **92**, 329 (1988).
[5] J. Segall, R. Lavi, Y. Wen, and C. Witting, J. Phys. Chem. **93**, 7287 (1989).
[6] P. G. Green, J. L. Kinsey, and R. W. Field, J. Chem. Phys. **91**, 5160 (1989).
[7] K. M. Ervin, S. Gronert, S. E. Barlow, M. K. Gilles, A. G. Harrison, V. M. Bierbaum, C. H. DePuy, W. C. Lineberger, and G. B. Ellison, J. Am. Chem. Soc. **112**, 5750 (1990).
[8] B. Ruscic and J. Berkowitz, J. Chem. Phys. **93**, 5586 (1990).
[9] D. P. Baldwin, M. A. Buntine, and D. W. Chandler, J. Chem. Phys. **93**, 6578 (1990).
[10] L. A. Curtiss and J. A. Pople, J. Chem. Phys. **91**, 2420 (1989).
[11] J. A. Montgomery, Jr. and G. A. Petersson, Chem. Phys. Lett. **168**, 75 (1990).
[12] C. W. Bauschlicher, Jr., S. R. Langhoff, and P. R. Taylor, Chem. Phys. Lett. **171**, 42 (1990).
[13] C. J. Wu and E. A. Carter, J. Am. Chem. Soc. **112**, 5893 (1990).
[14] For a discussion of complexities, see, e.g., H. Thümmel, M. Perić, S. D. Peyerimhoff, and R. J. Buenker, Z. Phys. D **13**, 307 (1989).
[15] R. F. Curl, P. G. Carrick, and A. J. Merer, J. Chem. Phys. **82**, 3479 (1985).
[16] P. D. Foo and K. K. Innes, Chem. Phys. Lett. **22**, 439 (1973).
[17] C. K. Ingold and G. W. King, J. Chem. Soc. **1953**, 2702.
[18] K. K. Innes, J. Chem. Phys. **22**, 863 (1954).
[19] M. Douay, R. Nietmann, and P. F. Bernath, J. Mol. Spectrosc. **131**, 261 (1988).
[20] K. P. Huber and G. Herzberg, *Molecular Spectra and Molecular Structure: IV. Constants of Diatomic Molecules* (Van Nostrand–Reinhold, New York, 1979).
[21] M. W. Chase, Jr., C. A. Davies, J. R. Downey, Jr., D. J. Frurip, R. A. McDonald, and A. N. Syverud, *JANAF Thermochemical Tables*, 3rd ed. (American Institute of Physics, New York, 1986).
[22] T. R. Fletcher and S. R. Leone, J. Chem. Phys. **90**, 871 (1989).
[23] J. R. McDonald, A. P. Baronavski, and V. M. Donnelly, Chem. Phys. **33**, 161 (1978).
[24] R. S. Urdahl, Y. Bao, and W. M. Jackson, Chem. Phys. Lett. **152**, 485 (1988).
[25] Y. Bao, R. S. Urdahl, and W. M. Jackson, J. Chem. Phys. **94**, 808 (1991).
[26] P. M. Goodwin and T. A. Cool, J. Mol. Spectrosc. **133**, 230 (1989).
[27] S. Shih, S. D. Peyerimhoff, and R. J. Buenker, J. Mol. Spectrosc. **64**, 167 (1977).
[28] S. Shih, S. D. Peyerimhoff, and R. J. Buenker, J. Mol. Spectrosc. **74**, 124 (1979).
[29] Y. T. Lee, J. D. McDonald, P. R. LeBreton, and D. R. Herschbach, Rev. Sci. Instrum. **40**, 1402 (1968); R. K. Sparks, Ph.D. thesis, University of California, Berkely, 1979.
[30] R. E. Continetti, B. A. Balko, and Y. T. Lee, J. Chem. Phys. **93**, 5719 (1990); R. E. Continetti, Ph.D. thesis, University of California, Berkeley, 1989.
[31] L. J. Kieffer, At. Data **1**, 19 (1969).
[32] X. Zhao, Ph.D. thesis, University of California, Berkeley, 1988.
[33] W.-B. Yan, J. L. Hall, J. W. Stephens, M. L. Richnow, and R. F. Curl, J. Chem. Phys. **86**, 1657 (1987).
[34] M. Vervloet and M. Herman, Chem. Phys. Lett. **144**, 48 (1988).
[35] P. G. Carrick, A. J. Merer, and R. F. Curl, Jr., J. Chem. Phys. **78**, 3652 (1983).
[36] H. Kanamori and E. Hirota, J. Chem. Phys. **89**, 3962 (1988).
[37] J. W. Stephens, W.-B. Yan, M. L. Richnow, H. Solka, and R. F. Curl, J. Mol. Struct. **190**, 41 (1988).
[38] K. Kawaguchi, T. Amano, and E. Hirota, J. Mol. Spectrosc. **131**, 58 (1988).
[39] H. Kanamori, K. Seki, and E. Hirota, J. Chem. Phys. **87**, 73 (1987).
[40] M. E. Jacox and W. B. Olson, J. Chem. Phys. **86**, 3134 (1987).
[41] T. A. Cool, P. M. Goodwin, and C. E. Otis, J. Chem. Phys. **93**, 3714 (1990).
[42] A lower value for $D_0(CC-H)$ has been determined since the initial writing of this paper by R. S. Urdahl, Y. Bao, and W. M. Jackson (Chem. Phys. Lett. **178**, 425 (1991). Using their $112.0 \pm 0.8$ kcal/mol would shift the assignments in Fig. 12 to translational energies 4 kcal/mol higher and would raise the estimates of the $C_2$ internal energy by 4 kcal/mol.